European Journal of Clinical Pharmacy
Print ISSN: 2385-409X **Online ISSN**: 3105-0409
Website: https://farmclin.com/

Original Research Article

An Insight into Bioactive Properties of Andrographis paniculata for Treating Urinary Tract Infection: An *In-silico* Approach

Article History:

Name of Author:
Lavanya Davangere Kumar[1], Poojitha Banuvalli Sridhara Setty [2], Chandrashekar Srinivasa[1], Sharanagouda Patil[3], Anil Kumar K M[4], Chandan Shivamallu[5], Bhargav Shreevatsa[6]*, Gopinath Shanbhog Mashewarappa[1]*

Affiliation: *[1]Department of Studies in Biotechnology, Davangere University, Shivagangotri Campus, Davangere, Karnataka, India.*
[2]Department of Biotechnology, G M Institute of Technology, Davangere, Karnataka, India.
[3]ICAR - National Institute of Veterinary Epidemiology and Disease Informatics, Bengaluru, Karnataka, India.
[4]Department of Environmental Science, School of Life Sciences, JSS Academy of Higher Education & Research, SS Nagar, Mysuru-570015, Karnataka, India
[5]Department of Biotechnology and Bioinformatics, JSS Academy of Higher Education and Research, Mysuru, Karnataka, India.
[6]Department of Microbiology, JSS Academy of Higher Education and Research, Mysuru, Karnataka, India.

Corresponding Author:
Prof. Gopinath Shanbhog Mashewarappa

Received: 12-11-2025
Revised: 25-11-2025
Accepted: 10-12-2025
Published: 25-12-2025

Abstract: Urinary tract infections (UTIs) affect more than 150 million individuals worldwide each year. Escherichia coli is typically the primary causative agent of UTIs, while Klebsiella pneumoniae and *Staphylococcus aureus* are often implicated as secondary pathogens. The rising prevalence of multidrug resistance and biofilm-associated pathogenicity has made the treatment of UTIs increasingly challenging. In this study, we evaluated the anti-biofilm potential of Andrographis paniculata, a medicinal plant known for its anti-inflammatory and antimicrobial properties, using an *in silico* approach. Phytocompounds from *A. paniculata* were docked against three biofilm-associated target proteins: extended-spectrum beta-lactamase (ESBL) from *K. pneumoniae*, fibronectin-binding protein from *S. aureus*, and glycoprotein adhesin SasA from *Staphylococcus saprophyticus*. Molecular docking was performed using the Glide module of Schrödinger software, followed by molecular dynamics (MD) simulations, density functional theory (DFT) analysis, and pharmacokinetic profiling using ADMET. Among the compounds, quinic acid and andrographiside exhibited the strongest binding affinities towards ESBL (-7.948 and -7.825 kcal/mol, respectively), forming multiple hydrogen bonds with active site residues. MD simulations confirmed the stability of the quinic acid–fibronectin protein complex. DFT and ADMET analyses further validated the favorable electronic reactivity and low toxicity profiles of these phytocompounds. Collectively, our computational findings highlight *A. paniculata* phytoconstituents, particularly quinic acid, as promising lead candidates for the development of anti-biofilm therapies against drug-resistant pathogens associated with UTIs.

Keywords: UTI, *Andrographis Paniculate*, Anti-biofilm, Phytobioactives.

INTRODUCTION

Urinary tract infection (UTI) is one of the most common bacterial illnesses, affecting nearly 150 million people annually worldwide. UTIs typically occur due to infections of the bladder (cystitis) or the kidney (pyelonephritis), caused by bacterial colonization of the urinary tract, including the bladder and kidneys (Mancuso et al., 2023). *Klebsiella pneumoniae* and *Staphylococcus aureus* are important causative agents of UTIs, with a relatively higher capacity for biofilm formation compared to many other uropathogens. The ability to form biofilms contributes significantly to their pathogenicity and persistence. Biofilms are structured communities of bacteria encased within a self-secreted extracellular polymeric substance (EPS) matrix that can attach to both biotic and abiotic surfaces (Guerra MES, et al, 2022). Within this protective matrix, bacteria are shielded from antimicrobial agents and the host immune response, thereby facilitating chronic infection. Biofilm formation enhances antibiotic resistance, restricts drug penetration, reduces therapeutic efficacy, and increases the persistence and severity of UTIs. In urine, biofilm formation may be induced; however, the direct correlation between biofilms and UTI prevalence remains an area of active investigation (Liu et al., 2024).

The clinical burden of biofilms is particularly evident in catheterized patients, where continuous colonization leads to recurrent infections, chronic inflammation, and increased morbidity. *K. pneumoniae* is a major pathogen associated with healthcare-associated and community-acquired UTIs. Its resistance mechanisms include the production of extended-spectrum beta-lactamases (ESBLs), enzymes that hydrolyze beta-lactam antibiotics such as penicillins and cephalosporins. ESBL-producing *K. pneumoniae* strains exhibit high levels of resistance, limiting therapeutic options, while the emergence of carbapenemase-producing strains has further exacerbated multidrug resistance (Paczosa et al., 2016) .

Biofilm development is a key survival strategy in such pathogens. The polysaccharide-rich EPS matrix stabilizes bacterial biofilms, protects cells from anti-microbials and host defenses, and enhances bacterial persistence and infectivity. In Escherichia coli, virulence factors such as fimbriae, capsules, adhesins, and quorum-sensing molecules contribute to biofilm structure and adhesion to uroepithelial cells. Similarly, *K. pneumoniae* utilizes virulence-associated genes such as mrkA (fimbrial adhesin) and bssS (biofilm-stimulating signal), which regulate biofilm maturation and bacterial adhesion, thereby sustaining persistent urinary tract infections (Singh et al., 2021).
Likewise, *Staphylococcus aureus*, particularly methicillin-resistant *S. aureus* (MRSA), is a common opportunistic pathogen responsible for urinary tract infections (UTIs), especially in hospitalized and catheterized patients. *S. aureus* expresses fibronectin-binding proteins (FnBPA and FnBPB), which play a key role in biofilm formation by mediating adhesion to host surfaces (via fibronectin) as well as abiotic surfaces such as catheters. These fibronectin-binding proteins enable *S. aureus* cells to adhere to fibrinogen, elastin, and fibronectin, thereby diminishing host immune responses and promoting bacterial aggregation. This process results in the establishment of stable, often irreversible biofilms. By facilitating bacterial clustering and protection, FnBPs enhance the survival capacity of *S. aureus*, enabling resistance against both immune responses and antibiotic treatments, thus contributing to chronic and recurrent infections (Tong et al., 2015).

At the molecular level, *S. aureus* biofilm formation is further regulated by the icaADBC operon, which encodes polysaccharide intercellular adhesin (PIA). PIA promotes intercellular attachment, thereby reinforcing biofilm development and persistence. The drug delivery barriers posed by biofilm-associated resistance mechanisms in both *K. pneumoniae* and *S. aureus* present a significant clinical challenge (Ahmad et al., 2022). The extracellular polymeric substance (EPS) matrix acts as both a physical and chemical shield, reducing antibiotic penetration and limiting the effectiveness of antimicrobial therapies. Consequently, conventional antimicrobial treatments, including standard prescription regimens, often fail to eradicate biofilms from colonized anatomical surfaces. This underscores the urgent need for alternative strategies to effectively disrupt biofilm growth (Gunn et al., 2016).

Phytochemicals derived from medicinal plants, such as Andrographis paniculata (commonly known as “King of Bitters”), represent a promising avenue of investigation. *A. paniculata* contains bioactive compounds with documented antimicrobial, antiinflammatory, and anti-biofilm properties (Alberts et al., 2025). In the present study, we focused on the potential of *A. paniculata* phytoconstituents to target biofilm-forming UTI pathogens, with the aim of enhancing antimicrobial efficacy. Specifically, we explored biofilm-associated proteins, including extended-spectrum beta-lactamase (ESBL) in *K. pneumoniae* and fibronectin-binding proteins in *S. aureus*, to better understand resistance mechanisms and identify new therapeutic leads. Unraveling the molecular interactions between phytocompounds and bacterial biofilm regulators may provide a foundation for the development of plant-based therapies to combat biofilm-associated UTIs (Sah et al., 2019)

MATERIALS AND METHODS

Retrieval of Phytocompounds

Phytochemical constituents of Andrographis paniculata were retrieved from the Indian Medicinal Plants, Phytochemistry and Therapeutics (VivekAnanth et al., 2023) (IMMPAT) database (https://cb.imsc.res.in/immpat/), a curated resource that includes phytochemicals from over 1,700 Indian medicinal plants. Compounds associated with *A. paniculata* were downloaded in SMILES and SDF formats for further analysis (Shreevatsa et al., 2024). The list of phytobioactives of *Andrographis Paniculate* are mentioned in Table 1.

Protein Selection and Preparation

The three-dimensional crystal structures of Glycoprotein adhesin SasA (PDB ID: 3IRP), Fibronectin (PDB ID: 4B60), and ESBL protein (PDB ID: 3OPL) were retrieved from the RCSB Protein Data Bank (PDB). (Figure -1 shows the protein structures retrieved from RCSB Protein Data Bank.These structures were prepared using the protein preparation wizard of Maestro v13.3 to fix all the problems in the existing structures. The bond orders were assigned, hydrogen bonds optimized, and missing loops and side chains were filled using Prime. Additionally, water molecules were removed (Frau et al., 2021).

Binding Site Prediction

The binding sites of proteins were retrieved using the Sitemap tool of the Schrödinger Suite. The top-ranked potential binding site was selected in the receptor grid generation tool of the suite to generate a grid surrounding the binding site amino acid residues for both the proteins which generated grid zip files as the output (Shreevatsa et al., 2024).

Molecular Docking

Schrodinger Glide software (version) was employed to conduct the docking studies and visualize the docked complexes, ensuring precise interaction analysis. The phytobioactives were systematically docked against three key protein targets: Glycoprotein adhesin SasA, Fibronectin, and ESBL protein. These computational analyses aimed to identify potential binding affinities and interactions between the ligands
and the selected protein targets (Tsivileva et al., 2022)

ADMET

ADMET (Absorption, Distribution, Metabolism, Excretion and Toxicity) analysis was used to obtain the pharmacokinetic and safety profiles of *Andrographis paniculata's* major phytocompounds based on docking score and number of H-bonds. The phytocompounds were obtained from the IMMPAT database and the drug-like properties were evaluated using SwissADME based on Lipinski's Rule of Five.

Those compounds meeting the drug-likeness screening were then analyzed utilizing pkCSM to predict critical parameters for the assessment of absorption (intestinal absorption, permeability over Caco2), distribution (penetrating blood brain barrier, Volume of distribution), metabolism (interacting with CYP450), excretion (clearance, half-life), and toxicity (mutagenicity, hepatotoxicity, LD_{50}). This screening process was critically important in identifying nontoxic drug-like compounds that can be subject to further validation (Sah et al., 2019).

Density Functional Theory

Density Functional Theory (DFT) calculations were performed using the Schrödinger Suite to investigate the electronic properties and binding interactions of phytocompounds. The quantum mechanical calculations were conducted using the Jaguar module with the B3LYP hybrid functional and 6-31G basis set for geometry optimization and energy calculations. The molecular structures of phytocompounds were prepared using LigPrep, ensuring proper protonation states and tautomeric form (Lila et al., 2023).

Molecular Dynamic Simulations

In this study, molecular dynamics (MD) simulations were performed using the Schrödinger Suite's Desmond module to investigate the dynamic behavior and binding interactions of Glycoprotein, and Fibronectin, with Quinic Acid. The systems were prepared using the OPLS4 force field, solvated in an explicit TIP3P water model within an orthorhombic box, and neutralized with counterions. Energy minimization and equilibration were conducted under NPT and NVT ensembles at 300 K and 1 atm pressure, followed by a 200-ns production run to analyze stability and ligand-protein interactions (Pestana-Nobles et al., 2022).

Statistical Analysis

The selection of top phytocompounds for further analysis was based on docking scores, number of significant hydrogen bond interactions, and binding site plausibility. Docking results with binding energies below -5.5 kcal/mol and multiple hydrogen bonds with key active site residues were prioritized. Molecular dynamics simulation stability was assessed using root mean square deviation (RMSD) and root mean square fluctuation (RMSF) analyses over a 200 ns trajectory. Stable protein-ligand complexes exhibited RMSD deviations below 3.5 Å for the protein backbone and consistent ligand positioning. ADMET profiling employed established *in silico* tools with default thresholds for drug-likeness, absorption, distribution, metabolism, excretion, and toxicity properties. Compounds meeting drug-likeness criteria with acceptable predicted toxicity profiles were considered promising leads.

RESULTS

Protein-Ligand Interaction Analysis

A molecular docking study was carried out to analyze the binding interaction affinity and Hydrogen bond interactions between the various phytocompounds and the target proteins involved in the biofilm formation in *K. pneumoniae, S. aureus and S. saprophyticus*. The docking results indicated that, in the tested compounds of this study, D-(-)-Quinic acid had the most binding affinity (-7.948 kcal/mol) with the ESBL protein (3OPL) of *K. pneumoniae* with Hydrogen bond's interaction with GLU171, HIS164, and ARG178. Whereas, Andrographiside had a slightly lower affinity (-7.852 kcal/mol) with Hydrogen bond's interactions with GLU240, ARG241, and GLU171. Deoxyandrographolide had a binding of -6.915 kcal/mol and significant Hydrogen bond interaction with ARG178 and HIS164. But, the 14-Deoxyandrographoside showed a lesser affinity (-5.607 kcal/mol) with interactions involving ASP176. The weakest interaction was 5,7-Dihydroxy-2-(4-hydroxyphenyl)-4H-chromen-4-one (-2.373 kcal/mol) which had no significant Hydrogen bonds interaction. The standard drug Ciprofloxacin had a binding of -3.671 kcal/mol with only one Hydrogen bond's with HIS164. Overall, D-(-)-Quinic acid and Andrographiside displayed the most binding affinity (-7.948 and -7.852 kcal/mol respectively), with a very extensive Hydrogen bonds interactions with ESBL protein. These two compounds may next be evaluated to verify as inhibitors inhibitor of ESBL proteins. The docking results of ESBL protein of *K. pneumoniae* with phytocompounds of *Andrographis paniculata* are mentioned in Table 2.

Interaction of Phytocompounds with Fibronectin Protein (4B60) of *Staphylococcus aureus*

The docking study of Fibronectin (4B60) exhibited significant interactions with the diverse phytocompounds. The standard drug Linezolid had a binding energy of -7.348 kcal/mol forming 2 hydrogen bonds with TYR501 and HIS254. Quinic Acid had six hydrogen bonds with SER351, ASN496, GLY497, and VAL499 yielding a binding energy of -6.928 kcal/mol, thus emerging as a very candidate. Andrographiside had a binding energy of -6.641 kcal/mol via three hydrogen bonds with GLY497, ASN496 and GLU353. Oroxylin A and Apigenin also exhibited binding affinities of -6.743 kcal/mol and -5.989 kcal/mol. Taken together, the analyses of Quinic Acid and Linezolid exhibited the greatest potentials to inhibit biofilm formation in *S. aureus*. The docking result of Fibronectin protein of *Staphylococcus aureus* with phytocompounds of *Andrographis Paniculate* are mentioned in Table 3.

Interaction of Phytocompounds with Glycoprotein Adhesin SasA (3IRP) of *Staphylococcus saprophyticus*

Molecular docking results for the Glycoprotein adhesin SasA (3IRP) revealed that Ampicillin, the standard drug, exhibited a binding affinity of -5.816 kcal/mol, forming two hydrogen bonds with ASN466 and ASN752. Apigenin showed the highest binding affinity (-7.886 kcal/mol), forming hydrogen bonds with TYR755, ASN467, and TYR481. Quinic Acid displayed six hydrogen bonds with TYR755, ASN467, THR751, and ASN749, with a binding affinity of -6.223 kcal/mol. These results suggest that Apigenin and Quinic Acid could be potential inhibitors of biofilm formation in *S. saprophyticus.* The Docking result of Glycoprotein adhesin SasA of *Staphylococcus saprophyticus* with phytocompounds of *Andrographis paniculata* are mentioned in Table 4.

The docking analysis presented in this study provided good interactions between the compounds and the target protein (eg., 1E0I), and emphasizes their use in future studies as beneficial therapeutic agents. Andrographiside displayed three hydrogen bonds with GLY-497, ASN-496, and GLU-353, it displayed a binding affinity of -6.641 kcal/mol. Quinic Acid displayed six hydrogen bonds with SER-351, ASN-496, GLY-497, and VAL-499, and had a binding affinity of -6.928 kcal/mol and provided good lead against the complete typological structure. With Oroxylin A, it displayed a single hydrogen bond with GLY-497, and a binding affinity of -6.743 kcal/mol, Apigenin displayed three hydrogen bonds with PRO-219, VAL-499, and TYR-501 and a binding affinity of -5.989 kcal/mol. 5,2'Dihydroxy-6,7,8,6'-tetramethoxyflavone two hydrogen bonds with GLY-497, and VAL-499 and had a binding affinity of -6.184 kcal/mol. Finally, Andrographidine A, displayed three hydrogen bonds with HIS-254, GLU-353, and ARG-260 and a binding affinity of -5.831 kcal/mol. Linezolid (standard) interacted with two hydrogen bonds with TYR-501 and HIS-254, with a binding affinity of -7.348 kcal/mol. Based on favorable binding affinity and effective hydrogen bonding, future studies should consider investigating the molecules, Linezolid and Quinic Acid selectivity since they show potent hydrogen bonding and strong binding affinities.

ADMET studies of the selective phytocompounds

The ADMET (Absorption, Distribution, Metabolism, Excretion, and Toxicity) studies were performed to examine the pharmacokinetic properties and possible toxicity characteristics of the identified phytocompounds. Many drug development efforts fail because of polymorphic ADMET properties, so to assess bioavailability and drug-likeness, *in silico* screening was used, which showed the screened compounds had good ADMET profiles with small amounts of toxicity, making them

relevant candidates to be selected for drug development studies. This detail is available in Table 5, which highlights the ADMET analysis findings.

Density Functional Theory

In the current Density Functional Theory (DFT) analysis, the phytobioactive compound Quinic acid was subjected to quantum chemical calculations in order to determine the electronic properties and chemical reactivity. Figure 2 represents. The energy levels of the HOMO and LUMO were calculated to be -0.25671 eV and -0.0021 eV, respectively, yielding a HOMO-LUMO energy gap of -0.297751 eV. This energy gap is relatively small and therefore implies only moderate electronic stability of Quinic acid and higher potential chemical reactivity, which is favorable to biological interactions. The HOMO localization shows electron-rich regions over the oxygenated functional groups, while the LUMO distribution indicates that the concentrated charge density is at electrophilic centers suggesting active sites where nucleophilic and electrophilic attacks may occur. Similarly, electrostatic potential (ESP) mapping shows charge distribution of the molecule where red ESP zones represent high electron density regions and blue ESP zones represent electron-poor regions. Overall, it appears that Quinic acid has electronic properties suitable for productive interaction with biological targets such as topoisomerases.

Molecular Dynamics Simulation

The Root Mean Square Deviation (RMSD) and Root Mean Square Fluctuation (RMSF) analyses were conducted to assess the structural stability and residue-level flexibility of both glycoprotein and fibronectin complexed with quinic acid over the 200 ns molecular dynamics simulation. RMSD for glycoprotein (A) indicated stability with minimal deviations of mostly < 3.5 Å for the protein backbone; quinic acid, although it exhibited greater mobility at the start of the timeline (t = 0-100 ns), a significant deviation was observed at t = 150 ns, indicating a stable binding interaction. For fibronectin (B), both the protein (with RMSD values varying ~2.0 - 2.5 Å) and ligand (2.0 - 5.0 Å) RMSD remain stable, indicating the flexible, yet, stable interactions. The RMSF plots for glycoprotein (C) and fibronectin (D) presented regions of high flexibility within specific regions, primarily in loop regions; the ligand contact points (green) generally appeared within stable or moderately flexible sections of the protein backbone. Overall, these results show quinic acid has stable interactions with both targets with particularly strong interactions in known ligand binding pockets contributing to overall stability and conformational retention of the drug complex during the simulation. (Figure 3)

Table 1:List of phytobioactives of *Andrographis Paniculate.*

Sl.No.	Phytochemical	Structure	Part of Plants
01.	Andrographiside	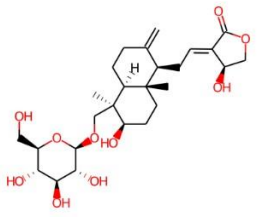	Whole plant
02.	Andrograpanin	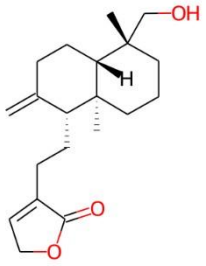	Aerial part, leaf, whole plant

03.	Andrographolide	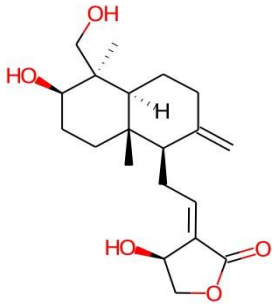	Aerial part, leaf, rhizome, root
04.	14-Deoxy-11,12didehydroandrographolide	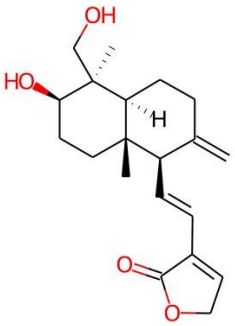	Aerial part
05.	Neoandrographolide	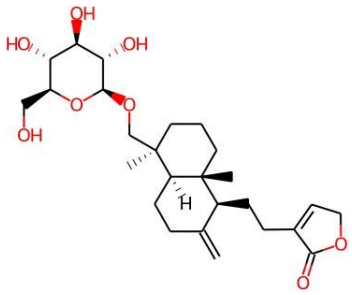	Aerial part
06.	Andrographin	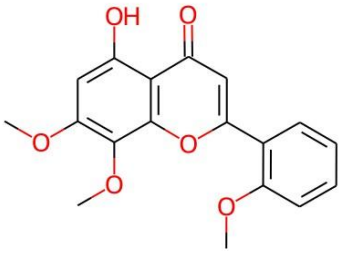	Leaf, Root

07.	Deoxyandrographolide	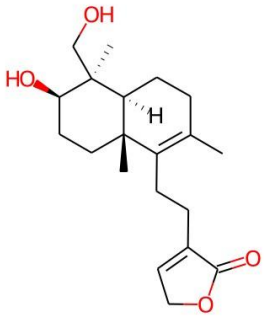	Leaf, Rhizome
08.	5-Hydroxy-7,8-dimethoxyflavone	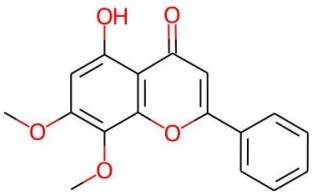	Leaf, Root
09.	Quinic acid	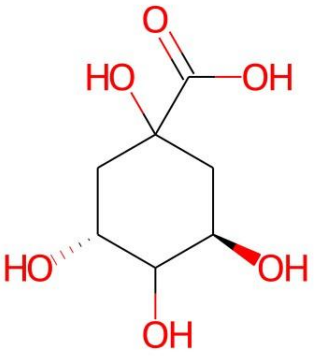	Leaf
10.	alpha1-Sitosterol	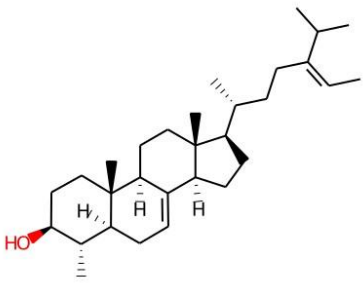	Leaf

11,12.	Chlorogenic acid	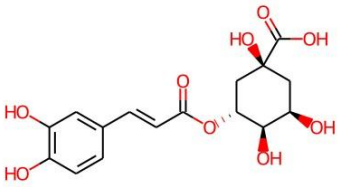	Leaf
13.	Caffeic acid	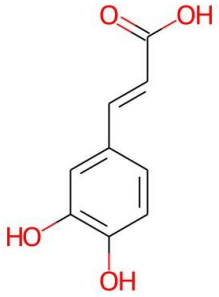	Leaf
14.	Daucosterol	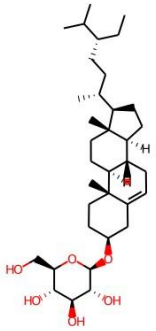	Leaf
15.	Andrographidine F	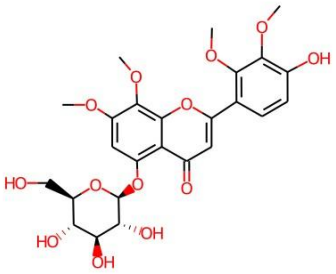	Root
16.	Andrographidine D	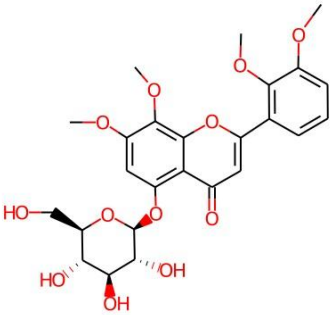	Root

17.	Andrographidine B	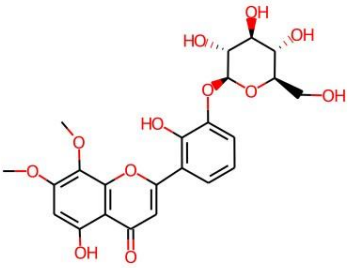	Root
18.	Andrographidin A	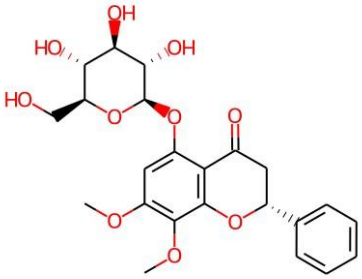	Root
19.	Skullcapflavone I	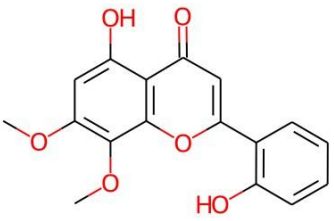	Root
20.	Andrographidine C	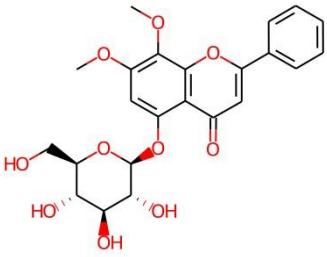	Root

21.	alpha1-Sitosterol	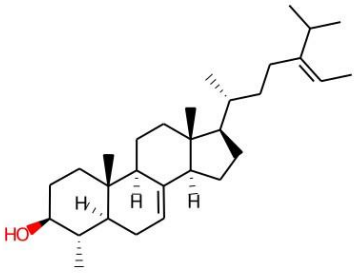	Root
22.	beta-Sitosterol	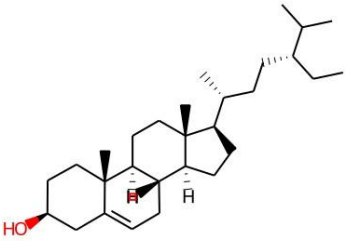	Root
23.	Andrographidine E	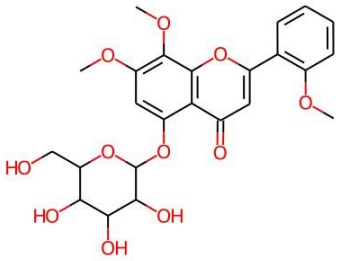	Root
24.	Myristic acid	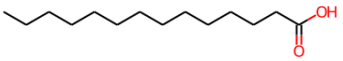	Whole plant

25.	14-Deoxy-12methoxyandrographolide	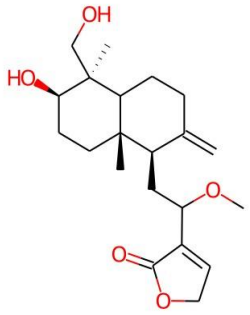	Whole plant
26.	Carvacrol	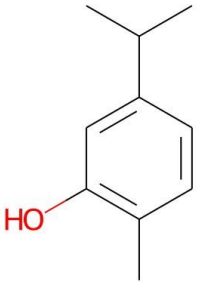	Whole plant
27.	Eugenol	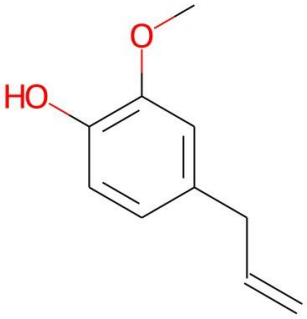	Whole plant
28.	Oroxylin A	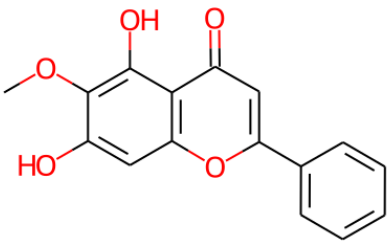	Whole plant

29.	Wogonin	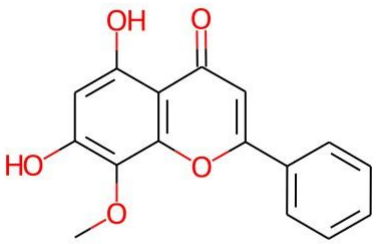	Whole plant
30.	Hentriacontane		Whole plant
31.	Andropanoside	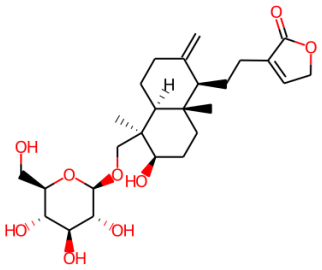	Whole plant
32.	Apigenin	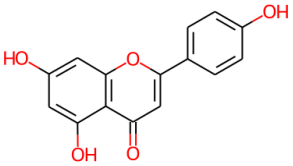	Whole plant

Table 2: Docking result of ESBL protein of *K. pneumoniae* with phytocompounds of *Andrographis paniculata.*

Sl. No.	Protein Name and ID	Molecule Name	H - Bond	Binding Energy (kcal/mol)	H-bond Amino Acids	Ligand Interaction
1	ESBL Protein (3OPL)	Ciprofloxacin – Standard Drug	1	-3.671	HIS – 164	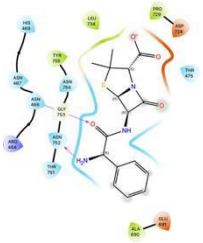
2		Quinic Acid	5	-7.948	GLU-171, HIS164, ARG-178	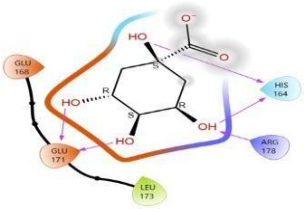
3		Andrographiside	5	-7.852	GLU-240, ARG-241, GLU-171	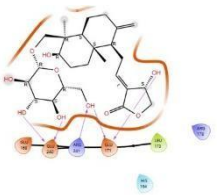
4		14-Deoxyandrographoside	2	-5.607	ASP-176	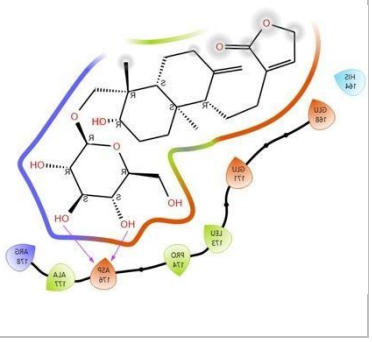

5		5,7-Dihydroxy-2-(4hydroxyphenyl)-4Hchromen-4-one	-	-2.373		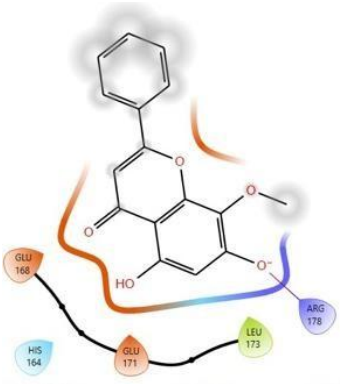
6		Deoxyandrographolide	3	-6.915	ARG-178, HIS-164	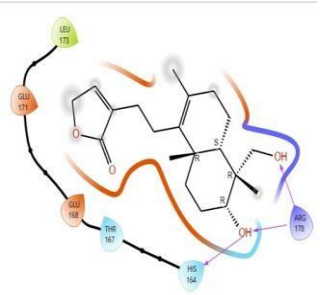

Table 3: Docking result of Fibronectin protein of *Staphylococcus aureus* with phytocompounds of *Andrographis Paniculate.*

Sl. No.	Protein Name and ID	Molecule Name	H - Bond	Binding Energy (kcal/mol)	Hbond Amino Acids	Ligand Interaction
1	Fibronectin (4B60)	Linezolid – Standard Drug	2	-7.348	TYR – 501, HIS254	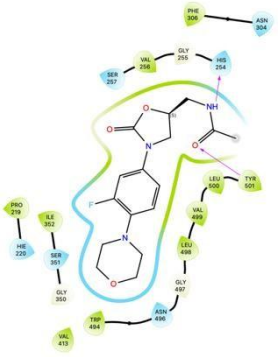

2		Andrographiside (44593583)	3	-6.641	GLY – 497, ASN-496 GLU - 353	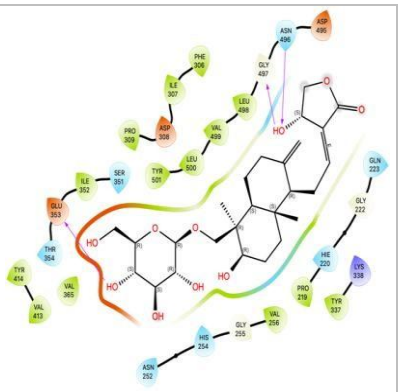
3		Quinic Acid (6508)	6	-6.928	SER – 351, ASN-496, GLY – 497, VAL - 499	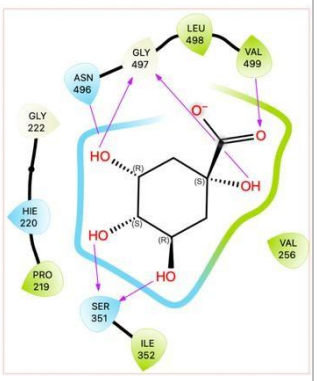
4		Oroxylin A (5320315)	1	-6.743	GLY-497	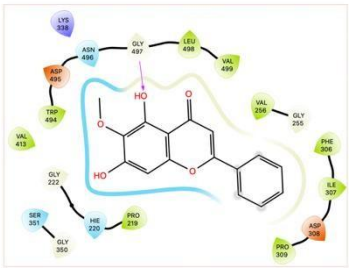
5		Apigenin (5280443)	3	-5.989	PRO – 219, VAL-499, TYR – 501,	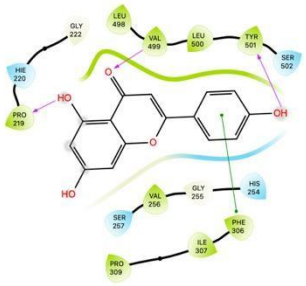
6		5,2'-Dihydroxy-6,7,8,6'tetramethoxyflavone (124211)	2	-6.184	GLY – 497, VAL - 499	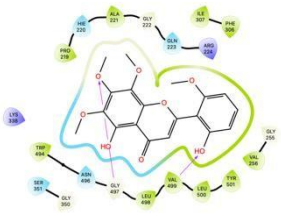

7		Andographidine A (13963762)	3	-5.831	HIS254, GLU-353, ARG-260	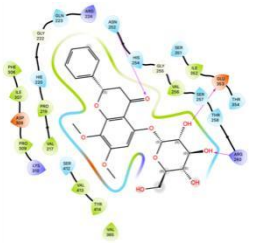

Table 5: ADMET identified properties of top phytobioactives of *Andrographics paniculata.*

ADMET Entry	Andrographiside	Andrographilode	Deoxyandrographolide	Quinic acid	Andrographidine	Andropanoside
Drug Likeness						
Lipinski	No	Yes	Yes	Yes	No	Yes
Bioavailability Score	0.17	0.55	0.55	0.56	0.55	0.55
Solubility						
Water Solubility	Yes	Yes	Yes	Yes	Yes	Yes
Absorption						
Intestinal Absorption	Low	High	High	Low	High	Low
Skin Permeability	-9.41	-6.9	-6.28	-9.15	5.9	-8.74
Pglycoprotein Substrate	No	No	Yes	Yes	No	No
Distribution						
BBB Permeability	No	No	Yes	No		No
CYP1SA2 Inhibitor	No	Yes	Yes	No		No
CYP12C19 Inhibitor	No	No	No	No		No
CYP2C9 Inhibitor	No	No	No	No		No

CYP2D6 Inhibitor	No	No	No	No		No
CYP3A4 Inhibitor	No	No	No	No		No
Toxicity						
AMES Toxicity	No	No	No	No		No

Figures:

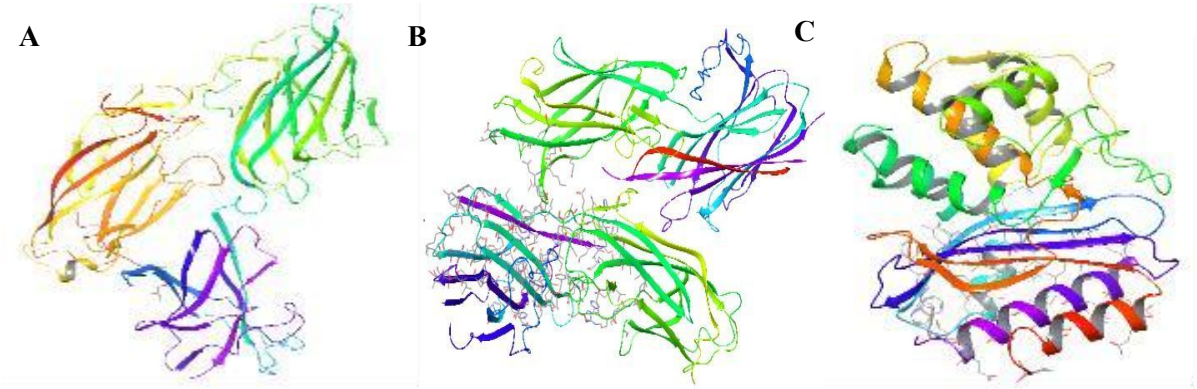

Figure 1: 3D Structure of Protein; (A) Glycoprotein Adhesin SasA (PDB ID: 3IRP); (B) Fibronectin (PDB ID: 4B60); (C) ESBL (PDB ID: 3OPL).

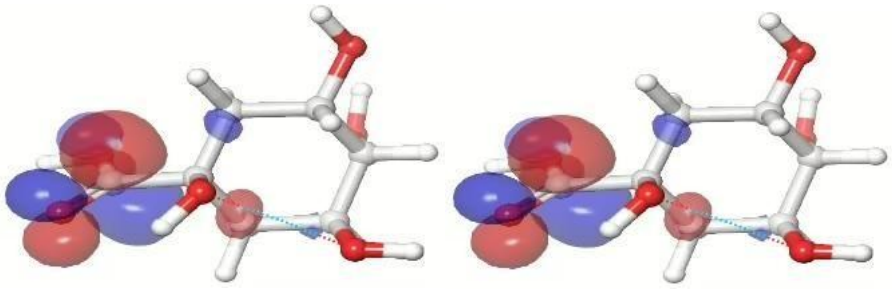

HOMO = – 0.25671 eV **LUMO = – 0.0021 eV**

C.

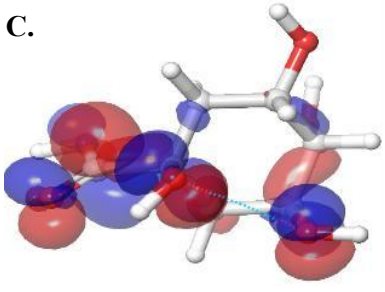

ESP = – 023571 eV

Figure 2:

Representation of (A) HOMO; (B) LUMO; (C)Electrostatic Potential (ESP) properties of the quinin acid.

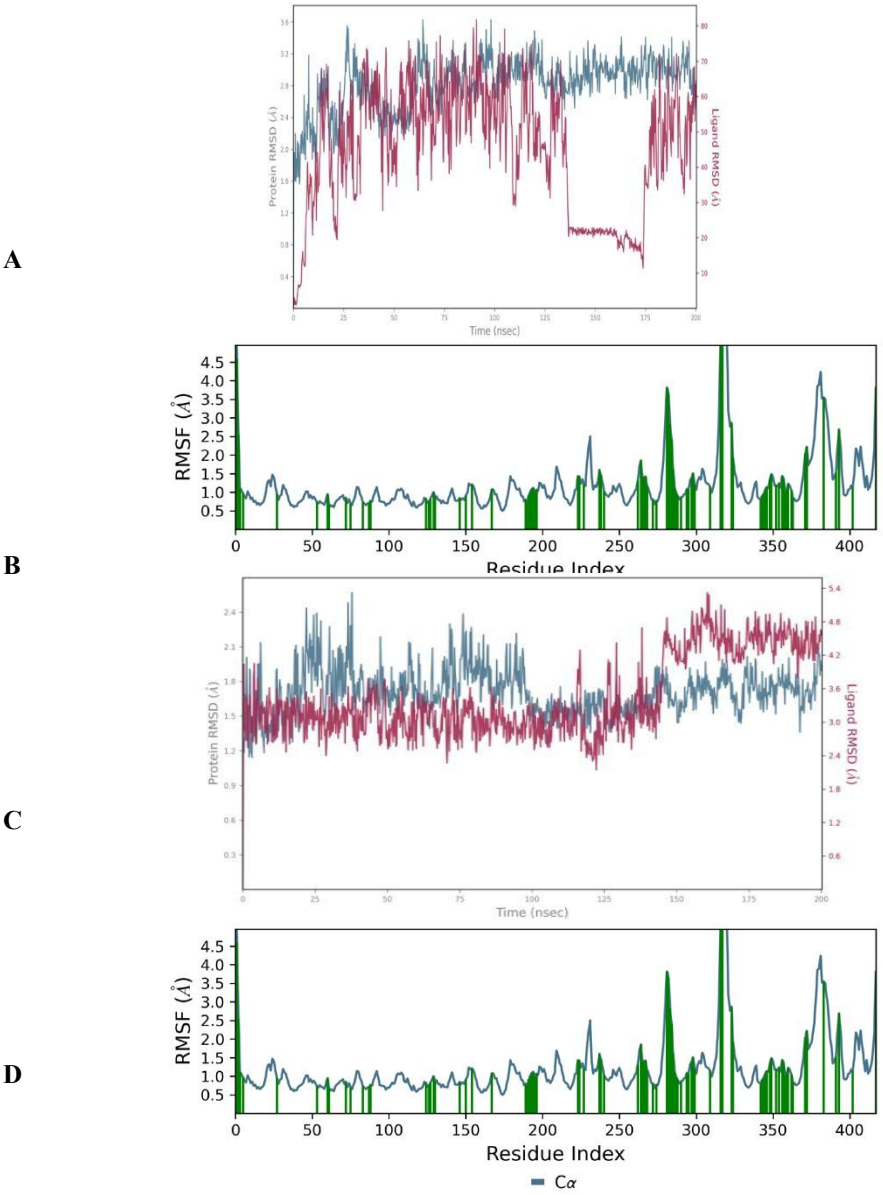

Figure 3: Root Mean Square Deviation (RMSD) of (A) Glycoprotein, and (B) Fibronectin, protein (blue) and (C, D) Quinic Acid ligand (red) in Angstroms (Å) against time and (C, D) Root Mean Square Fluctuations (RMSF) of proteins (Å) (blue) and ligand contact with the amino acids (green) against residue index.

DISCUSSION

In this study, we employed an *in silico* approach to investigate the potential anti-biofilm and antimicrobial activities of phytochemicals derived from *Andrographis paniculata* (family Acanthaceae) against major uropathogens implicated in urinary tract infections (UTIs), including *Klebsiella pneumoniae*, *Staphylococcus aureus*, and *Staphylococcus saprophyticus* (Guan et al., 2018).Our analysis primarily focused on biofilm formation, a critical virulence factor that underlies chronic and catheterassociated UTIs. Biofilms are regulated by quorum sensing (QS) pathways, which govern bacterial communication, adhesion, and biofilm maturation. Thus, disruption of QS-regulated proteins represents a promising therapeutic strategy. Among the compounds screened, quinic acid demonstrated the strongest binding affinity toward biofilm-associated target proteins, surpassing both standard antibiotics (e.g., ciprofloxacin, linezolid) and structurally related phytochemicals (Withana et al., 2025) Molecular docking revealed that quinic acid formed stable and energetically favorable interactions with proteins such as extended-spectrum β-lactamases (ESBLs) and fibronectin-binding proteins. These interactions suggest a potential mechanism of action through the inhibition of bacterial adhesion and

extracellular matrix formation, thereby impairing biofilm development.

Molecular dynamics (MD) simulations further substantiated the docking results by demonstrating the stability of hydrogen bond interactions between quinic acid and fibronectin-binding domains throughout the simulation period. The minimal root mean square fluctuation (RMSF) values observed in the Cα backbone of the protein confirmed the structural stability of the ligand–protein complex. Complementary Density Functional Theory (DFT) analysis supported these findings by highlighting the favorable electronic reactivity and stability of quinic acid, reinforcing its suitability as a potential bioactive molecule (Abdul-Hammed et al., 2021).

Pharmacokinetic profiling using ADMET (Absorption, Distribution, Metabolism, Excretion, and Toxicity) revealed that quinic acid and andrographiside possess acceptable drug-likeness and low predicted toxicity. However, limitations in oral bioavailability were noted for certain compounds, indicating the need for optimization through formulation or structural modification strategies. Taken together, these results suggest that phytochemicals from *A. paniculata* particularly quinic acid exhibit strong potential to interfere with QS-regulated pathways and adhesion mechanisms in biofilm-forming pathogens. By preventing the establishment and persistence of biofilms, these compounds may represent valuable leads for the development of alternative or adjunct therapies to combat chronic and catheter-associated UTIs. Importantly, this aligns with growing evidence that plant-based compounds offer a promising solution to the escalating problem of antimicrobial resistance. Despite these promising findings, this study is limited to computational predictions. Experimental validation, including **in vitro** and **in vivo** assays, is necessary to confirm the bioactivity, safety, and therapeutic efficacy of the identified compounds. Future research should also examine potential synergistic interactions between *A. paniculata* phytochemicals and conventional antibiotics, as well as strategies to improve their pharmacokinetic properties, particularly bioavailability.

CONCLUSION

This *in silico* investigation highlights quinic acid and related phytoconstituents from *Andrographis paniculata* as promising candidates for the development of antibiofilm therapies against urinary tract infection (UTI) pathogens. The computational analyses including molecular docking, molecular dynamics, density functional theory, and ADMET profiling collectively suggest that these compounds possess favorable binding affinities, stability, and acceptable pharmacokinetic properties. By targeting biofilm -associated regulatory proteins, such as extended-spectrum β-lactamases and fibronectin-binding proteins, these phytochemicals demonstrate the potential to disrupt bacterial adhesion and biofilm persistence. Overall, this work underscores the potential of *A. paniculata* phytochemicals, especially quinic acid, as lead molecules in the pursuit of next-generation antimicrobial and anti-biofilm therapies

.

ACKNOWLEDGEMENT

The authors LDK, CSS, GDSM acknowledge the support and infrastructure provided by Davangere University; BS, CS, acknowledge JSS AHER for the support extended for the *Schrodinger Suite* facility provided. SPK thanks Amrita Vishwa Vidyapeetham for support extended towards the collaborations. The Corresponding authors acknowledge Government of Karnataka for the funding support provided under the scheme of VGST/KFIST L1/GRD No. 878.

ABBREVIATIONS

UTI: Urinary Tract Infections; ESBL: Extended Spectrum Beta-Lactamase; MD: Molecular Dynamics; DFT: Density Functional Theory; ADMET: Absorption, Distribution, Metabolism, Excretion, and Toxicity; EPS: Extracellular Polymeric Substance; MRSA: Methicillin-Resistant *Staphylococcus aureus*; FnBPs: Fibronectin-Binding Proteins; PIA: Polysaccharide Intercellular Adhesin; IMMPAT: Indian Medicinal Plants, Phytochemistry
and Therapeutics

.

CONFLICT OF INTEREST

"The authors declared no potential conflicts of interest."

Author Contributions

Lavanya Davangere Kumar conceptualized the study, performed molecular docking and dynamics simulations, and drafted the manuscript. Poojitha Banuvalli Sridhara Setty contributed to data analysis and manuscript editing. Chandrashekar Srinivasa and Anil Kumar assisted in phytochemical retrieval and ADMET analysis. Bhargav Shreevatsa and supervised the study design and methodology, validated the docking protocols.
Sharanagouda Patil and Shiva Prasad Kollur provided resources and infrastructure support. Chandan Shivamallu contributed to quantum chemical calculations. Gopinath Shanbhog Mashewarappa supervised overall project administration and revised the manuscript critically. All authors reviewed and approved the final manuscript.

FUNDING STATEMENT

The research has been funded by the support of Government of Karnataka for the funding support

provided under the scheme of VGST/KFIST L1/GRD No. 878.

REFERENCES

1. Abdul-Hammed, M., Adedotun, I. O., Falade, V. A., Adepoju, A. J., Olasupo, S. B., & Akinboade, M. W. (2021). Target-based drug discovery, ADMET profiling and bioactivity studies of antibiotics as potential inhibitors of SARS-CoV-2 main protease (Mpro). *VirusDisease, 32*(4), 642–656. https://doi.org/10.1007/s13337-021-00717-z
2. Ahmad, S., Rahman, H., Qasim, M., Nawab, J., Alzahrani, K. J., Alsharif, K. F., & Alzahrani, F. M. (2022). *Staphylococcus epidermidis* pathogenesis: Interplay of icaADBC operon and MSCRAMMs in biofilm formation of isolates from pediatric bacteremia in Peshawar, Pakistan. *Medicina (Kaunas), 58*(11), 1510. https://doi.org/10.3390/medicina58111510
3. Alberts, A., Lungescu, I. A., Niculescu, A. G., & Grumezescu, A. M. (2025). Natural products for improving soft tissue healing: Mechanisms, innovations, and clinical potential. *Pharmaceutics, 17*(6), 758. https://doi.org/10.3390/pharmaceutics17060758
4. Frau, J., Flores-Holguín, N., Shivamallu, C., Kollur, S. P., & Glossman-Mitnik, D. (2021). Virtual screening for potential phytobioactives as therapeutic leads to inhibit NQO1 for selective anticancer therapy. *Molecules, 26*(22), 6863. https://doi.org/10.3390/molecules26226863
5. Guan, L., Yang, H., Cai, Y., Sun, L., Di, P., Li, W., Liu, G., & Tang, Y. (2018). ADMET-score – A comprehensive scoring function for evaluation of chemical druglikeness. *MedChemComm, 10*(1), 148–157. https://doi.org/10.1039/c8md00472b
6. Guerra, M. E. S., Destro, G., Vieira, B., Lima, A. S., Ferraz, L. F. C., Hakansson, A. P., Darrieux, M., & Converso, T. R. (2022). *Klebsiella pneumoniae* biofilms and their role in disease pathogenesis. *Frontiers in Cellular and Infection Microbiology, 12*, 877995. https://doi.org/10.3389/fcimb.2022.877995
7. Gunn, J. S., Bakaletz, L. O., & Wozniak, D. J. (2016). What's on the outside matters: The role of the extracellular polymeric substance of Gram-negative biofilms in evading host immunity and as a target for therapeutic intervention. *Journal of Biological Chemistry, 291*(24), 12538–12546. https://doi.org/10.1074/jbc.R115.707547
8. Lila, A. S. A., Rajab, A. A. H., Abdallah, M. H., Rizvi, S. M. D., Moin, A., Khafagy, E. S., Tabrez, S., & Hegazy, W. A. H. (2023). Biofilm lifestyle in recurrent urinary tract infections. *Life (Basel), 13*(1), 148. https://doi.org/10.3390/life13010148
9. Liu, H. Y., Prentice, E. L., & Webber, M. A. (2024). Mechanisms of antimicrobial resistance in biofilms. *NPJ Antimicrobial Resistance, 2*, 27. https://doi.org/10.1038/s44259-024-00046-3
11. Mancuso, G., Midiri, A., Gerace, E., Marra, M., Zummo, S., & Biondo, C. (2023). Urinary tract infections: The current scenario and future prospects. *Pathogens, 12*(4), 623. https://doi.org/10.3390/pathogens12040623
12. Paczosa, M. K., & Mecsas, J. (2016). *Klebsiella pneumoniae*: Going on the offense with a strong defense. *Microbiology and Molecular Biology Reviews, 80*(3), 629–661. https://doi.org/10.1128/MMBR.00078-15
13. Pestana-Nobles, R., Aranguren-Díaz, Y., Machado-Sierra, E., Yosa, J., Galan-Freyle, N. J., Sepulveda-Montaño, L. X., Kuroda, D. G., & Pacheco-Londoño, L. C. (2022). Docking and molecular dynamic of microalgae compounds as potential inhibitors of betalactamase. *International Journal of Molecular Sciences, 23*(3), 1630. https://doi.org/10.3390/ijms23031630
14. Sah, S. K., Rasool, U., & Hemalatha, S. (2019). *Andrographis paniculata* extract inhibit growth, biofilm formation in multidrug resistant strains of *Klebsiella pneumoniae*. *Journal of Traditional and Complementary Medicine, 10*(6), 599–604. https://doi.org/10.1016/j.jtcme.2019.02.006
15. Shreevatsa, B., Dharmashekara, C., Jain, A. S., et al. (2022). An insight into reactivity and bioactivity properties of quorum sensing peptides against PDE10A: A computational peptidology approach. *Journal of Molecular Modeling, 28*, 209. https://doi.org/10.1007/s00894-022-05176-x
16. Shreevatsa, B., Hegde, S., Narayan, P., Dharmashekar, C., Jain, A., Wani, T. A., Prabhuswamimath, S. C., Kollur, S. P., & Shivamallu, C. (2024). Targeting FAK, VEGF, and MTA1 proteins with *Terminalia elliptica*: A computational approach for anticancer activity. *Frontiers in Oncology, 14*, 1427632. https://doi.org/10.3389/fonc.2024.1427632
17. Singh, S., Datta, S., Narayanan, K. B., & Rajnish, K. N. (2021). Bacterial exopolysaccharides in biofilms: Role in antimicrobial resistance and treatments. *Journal of Genetic Engineering and Biotechnology, 19*, 140. https://doi.org/10.1186/s43141-021-00242-y
18. Tong, S. Y., Davis, J. S., Eichenberger, E., Holland, T. L., & Fowler, V. G. Jr. (2015). *Staphylococcus aureus*infections: Epidemiology, pathophysiology, clinical manifestations, and management. *Clinical Microbiology Reviews, 28*(3), 603–661. https://doi.org/10.1128/CMR.00134-14
19. Tosun, F., et al. (2023). Biological activities of the fruit essential oil, fruit, and root extracts of *Ferula*

*drudeana*Korovin, the putative Anatolian ecotype of the Silphion plant. *Plants, 12*(4), 830. https://doi.org/10.3390/plants12040830

20. Trautner, B. W., & Darouiche, R. O. (2004). Role of biofilm in catheter-associated urinary tract infection. Am J Infect Control. 2004 May;32(3):177-83. https://doi.org/10.1016/j.ajic.2003.08.005v
21. Tsivileva, O. M., Koftin, O. V., & Evseeva, N. V. (2022). Coumarins as fungal metabolites with potential medicinal properties. *Antibiotics, 11*, 1156. https://doi.org/10.3390/antibiotics11091156
22. Vivek-Ananth, R. P., Mohanraj, K., Sahoo, A. K., & Samal, A. (2023). IMPPAT 2.0: An enhanced and expanded phytochemical atlas of Indian medicinal plants. *ACS Omega, 8*, 8827–8845. https://doi.org/10.1021/acsomega.3c00112
23. Withana, T. N., Perera, D., & Fernando, T. D. (2025). Molecular docking and drug-likeness of *Salicornia*-derived phytochemicals against HER receptors. *Current Issues in Molecular Biology, 47*, 495. https://doi.org/10.3390/cimb47070495

